Polymerizable Complex Synthesis of Pure $Sr_2Nb_xTa_{2-x}O_7$ Solid Solutions with High Photocatalytic Activities for Water Decomposition into H_2 and O_2

Mayu Yoshino and Masato Kakihana*

Materials and Structures Laboratory, Tokyo Institute of Technology, 4259 Nagatsuta, Midori-ku, Yokohama 226-8503, Japan

Woo Seok Cho

R&D Center, Samsung Corning Co., Ltd., 472 Shin-Dong, Paldal-gu, Suwon-City, Kyunggi-Do 442-390, Korea

Hideki Kato and Akihiko Kudo

Department of Applied Chemistry, Faculty of Science, Science University of Tokyo, 1-3 Kagurazaka, Shinjuku-ku, Tokyo 162-8601, Japan

Received September 21, 2001. Revised Manuscript Received May 6, 2002

Phase-pure solid solutions with the composition of $Sr_2Nb_xTa_{2-x}O_7$ (SNT, $x = 0-2$) were prepared at 900 °C for 5 h by the Pechini-type polymerizable complex (PC) technique, based upon polymerization between citric acid and ethylene glycol. The two end compounds, $Sr_2Ta_2O_7$ ($x = 0$) and $Sr_2Nb_2O_7$ ($x = 2$), produced H_2 and O_2 in a stoichiometric ratio from pure water under UV light irradiation without a NiO cocatalyst. The photocatalytic activity of SNT for the water decomposition was greatly improved by loading NiO as a cocatalyst for a whole range of x. The photocatalytic activity was dramatically decreased approximately by 1 order of magnitude once Ta has been replaced by Nb, even when the amount of Nb was small. For all of the NiO-loaded SNT samples, water was stoichiometrically decomposed into H_2 and O_2. While samples prior to the complete crystallization showed very low activities despite their high surface area, the corresponding photocatalytic activities of well-crystallized samples depended primarily on their surface area. The low photocatalytic activities of such premature samples were interpreted as a consequence of the increased number of lattice defects acting as inactivation centers. The maximum photocatalytic activity was obtained for NiO (0.15 wt %)/$Sr_2Ta_2O_7$ prepared by the PC method at 800 °C for 48 h; the photocatalyst having a specific surface area of 10.4 $m^2 \cdot g^{-1}$ produced H_2 and O_2 from pure water with specific rates of 3517 and 1733 $\mu mol \cdot h^{-1} \cdot g^{-1}$, respectively, 3.5 times larger than the best result for a sample prepared by the conventional solid-state reaction method.

Introduction

Heterogeneous photocatalytic reactions at semiconductor surfaces represent a very active research field. Among various interesting reactions, the photoinduced decomposition of water into H_2 and O_2 is potentially one of the most promising means for the conversion of photon energy into chemical energy.[1,2] Recently, Kudo and Kato have discovered high photocatalytic activities for the water decomposition in some alkaline and alkaline earth tantalates, which include $K_3Ta_3Si_2O_{13}$,[3] $BaTa_2O_6$,[4] $NaTaO_3$,[5−7] $SrTa_2O_6$,[8] $Sr_2Ta_2O_7$,[9] and $K_2LnTa_5O_{15}$.[10]

The vast majority of powder syntheses of these tantalates to date has been carried out using the conventional solid-state reaction (SSR) route at high temperatures (typically 1000−1300 °C). Common problems in the SSR route include the uncontrollably large grain growth, localized segregation of one or more components, and possible loss of stoichiometry due to volatilization of the constituent components at high temperatures, all of which result in a decrease in the photocatalytic activity of a given catalyst to a great extent. Considering the need to obtain pure and homogeneous crystalline powders with high surface areas for catalytic applications, solution processing is expected to

* To whom correspondence should be addressed. E-mail: kakihana@rlem.titech.ac.jp.

(1) Domen, K.; Kondo, J. N.; Hara, M.; Takata, T. *Bull. Chem. Soc. Jpn.* **2000**, *73*, 1307.
(2) Kudo, A. *J. Ceram. Soc. Jpn.* **2001**, *109*, S81.
(3) Kudo, A.; Kato, H. *Chem. Lett.* **1997**, 867.
(4) Kato, H.; Kudo, A. *Chem. Phys. Lett.* **1998**, *295*, 487.
(5) Kato, H.; Kudo, A. *Catal. Lett.* **1999**, *58*, 153.
(6) Kato, H.; Kudo, A. *J. Phys. Chem. B* **2001**, *105*, 4285.
(7) Kudo, A.; Kato, H. *Chem. Phys. Lett.* **2000**, *331*, 373.
(8) Kato, H.; Kudo, A. *Chem. Lett.* **1999**, 1207.
(9) Kudo, A.; Kato, H.; Nakagawa, S. *J. Phys. Chem. B* **2000**, *104*, 571.
(10) Kudo, A.; Okutomi, H.; Kato, H. *Chem. Lett.* **2000**, 1212.

10.1021/cm0109037 CCC: $22.00
Published on Web 07/20/2002

be satisfactory and the best adapted. We have previously developed the Pechini-type polymerizable complex (PC) route,[11−16] based upon polyesterification between citric acid and ethylene glycol, which was successfully applied to produce photocatalysts with improved activities for the decomposition of water when compared with those for samples prepared by the SSR method at high temperatures.[17−20]

The principal aim of this paper is to demonstrate the feasibility of the PC route for the low-temperature synthesis of tantalate-based materials with greater photocatalytic activities. Solid solutions of $Sr_2Nb_xTa_{2-x}O_7$ possessing layered perovskite structures[21,22] have then been chosen as the focus of the present work. This is because $Sr_2Ta_2O_7$ ($x = 0$) combined with NiO as well as NiO-loaded $NaTaO_3$ is a material which is attracting an increasing interest as a photocatalyst for water decomposition into H_2 and O_2 with outstandingly high activities.[5−7,9] While $Sr_2Ta_2O_7$ ($x = 0$) and $Sr_2Nb_2O_7$ ($x = 2$) in $Sr_2Nb_xTa_{2-x}O_7$ have been synthesized so far by the SSR method at 1180 °C for 200 h and at 1100 °C for 150 h,[9] the PC method was successfully applied to their synthesis typically at 900 °C for 5 h or at 800 °C for 48 h.

This paper describes the details of the PC synthesis of $Sr_2Nb_xTa_{2-x}O_7$, photocatalytic decomposition of water into H_2 and O_2 over $Sr_2Nb_xTa_{2-x}O_7$ with and without NiO, and effects of preparation temperature, heat-treatment time, and the amount of NiO loaded on the photocatalytic activities. The results are compared with those reported for samples prepared by the conventional SSR method.

Experimental Section

(a) Preparation of $Sr_2Nb_xTa_{2-x}O_7$. Powders of $Sr_2Nb_xTa_{2-x}O_7$ with $x = 0$, 0.1, 0.2, 0.3, 0.5, 0.7, 1.0, 1.5, and 2.0 were prepared by the PC method, as outlined in Figure 1. $SrCO_3$, $NbCl_5$, and $TaCl_5$ were chosen as starting metal sources. Ethylene glycol (EG) and methanol (MeOH) were used as solvents, and anhydrous citric acid (CA) was used as a chelating agent to stabilize Sr, Nb, and Ta ions. $NbCl_5$ and $TaCl_5$ were first dissolved in MeOH, followed by the addition of CA and EG with continuous stirring at 100 °C. After achieving complete dissolution, $SrCO_3$ was added and the mixture was stirred at 100 °C until it became a transparent colorless solution. The solution thus prepared, while stirred with a magnetic stirrer, was heated at ∼130 °C to promote polymerization between CA and EG. During the continued reaction at 130 °C, the solution became more viscous with time, and finally after several hours a brown resin-like gel was obtained without any visible precipitation. The brown gel was heated at 450 °C for several hours to remove residual solvents and to burn out unnecessary organics, while the solid matter was lightly ground into a powder by a Teflon rod all of the time. The powder thus obtained is referred to as powder precursors for $Sr_2Nb_xTa_{2-x}O_7$. Note that there is no chance to lose Sr or Ta (Nb) ions throughout our PC procedures, because all of the procedures in the PC method are carried out in one batch until the powder precursor has been obtained (Figure 1). This can guarantee no deviation from the initially fixed metal composition in the starting solution.

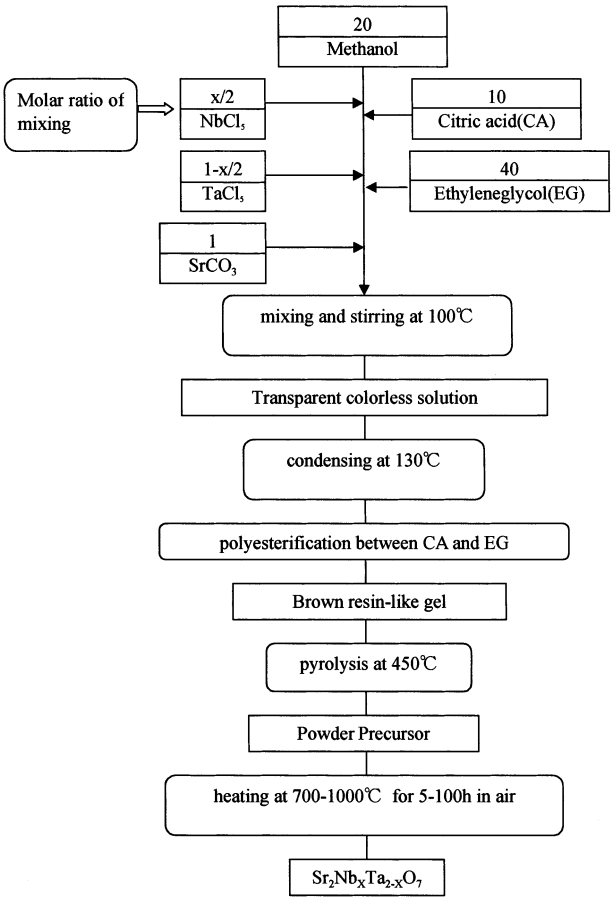

Figure 1. Flowchart for the polymerizable complex procedures used to prepare $Sr_2Nb_xTa_{2-x}O_7$ ($x = 0−2$) powders.

The powder precursor put on an Al_2O_3 crucible was heat-treated in a furnace at temperatures between 700 and 1000 °C for 5−100 h in air. Because no volatile metal components at the preparation temperatures are involved in the powder precursor, the initially prepared metal composition in the starting solution can be kept also in the final products.

(b) Preparation of NiO/$Sr_2Nb_xTa_{2-x}O_7$. NiO-loaded $Sr_2Nb_xTa_{2-x}O_7$ materials were made by the impregnation of powders of the host $Sr_2Nb_xTa_{2-x}O_7$ compounds with aqueous solutions of nickel nitrate, followed by appropriate heat treatments.[23] Powders of $Sr_2Nb_xTa_{2-x}O_7$ prepared by the PC method were suspended into an aqueous solution containing $Ni(NO_3)_2$ with a required amount, and it was evaporated to dryness on a water bath. The residue was heated in a crucible for 30 min by using a gas burner. The impregnated $Sr_2Nb_xTa_{2-x}O_7$ was heat-treated at 370 °C in a furnace for 1 h.

(c) Characterization. The products were characterized by X-ray diffraction (XRD) with a scanning speed of 4° min^{-1} for phase identification (MXP^{3VA}, Cu Kα, 40 kV−40 mA, MAC

(11) Pechini, M. P. U.S. Patent, No. 3,330,697, 1967.
(12) Eror, N. G.; Anderson, H. U. *Mater. Res. Soc. Proc.* **1986**, *73*, 571.
(13) Anderson, H. U.; Pennell, M. J.; Guha, J. P. In *Advances in Ceramics: Ceramic Powder Science*; Messing, G. L., Mazdiyasni, K. S., McCauley, J. W., Harber, R. A., Eds.; American Ceramic Society: Westerville, OH, 1987; Vol. 21, p 91.
(14) Lessing, P. A. *Am. Ceram. Soc. Bull.* **1989**, *168*, 1002.
(15) Kakihana, M. *J. Sol-Gel Sci. Technol.* **1996**, *6*, 7.
(16) Kakihana, M.; Yoshimura, M. *Bull. Chem. Soc. Jpn.* **1999**, *72*, 1427.
(17) Kakihana, M.; Domen, K. *MRS Bull.* **2000**, *25*, 27.
(18) Yamashita, Y.; Yoshida, K.; Kakihana, M.; Uchida, S.; Sato, T. *Chem. Mater.* **1999**, *11*, 66.
(19) Ikeda, S.; Hara, M.; Kondo, J. N.; Domen, K.; Takahashi, H.; Okubo, T.; Kakihana, M. *Chem. Mater.* **1998**, *10*, 72.
(20) Takahashi, H.; Kakihana, M.; Yamashita, Y.; Yoshida, K.; Ikeda, S.; Hara, M.; Domen, K. *J. Alloys Compd.* **1999**, *285*, 77.
(21) Ishizawa, N.; Marumo, F.; Kawamura, T.; Kimura, M. *Acta Crystallogr.* **1975**, *B31*, 1912.
(22) Ishizawa, N.; Marumo, F.; Kawamura, T.; Kimura, M. *Acta Crystallogr.* **1976**, *B32*, 2564.
(23) Kudo, A.; Sayama, K.; Tanaka, A.; Asakura, K.; Domen, K.; Maruya, K.; Onishi, T. *J. Catal.* **1989**, *120*, 337.

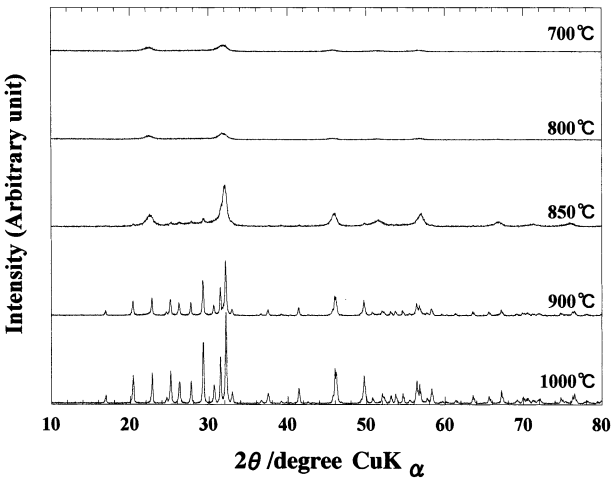

Figure 2. XRD patterns of $Sr_2Ta_2O_7$ synthesized by the polymerizable complex method at various temperatures (700−1000 °C) for 5 h.

Science). The specific surface area of the samples (1.0 g of each) was measured by the conventional Brunauer−Emmett−Teller (BET) method (Coulter, SA3100). Ultraviolet−visible (UV−vis) diffuse reflectance spectra were measured for the products using a JASCO UbsetV-570 spectrometer, and they were converted from reflection to absorbance through the standard Kubelka−Munk method. Observations of $Sr_2Ta_2O_7$ particles by transmission electron microscopy (TEM) were performed with a JEOL JEM-2010 electron transmission microscope operated at 200 kV.

Photocatalytic reactions were carried out in a closed-gas circulation system. The powdered photocatalysts (0.7 g of each) were magnetically suspended in 350 mL of pure water in an inner irradiation quartz cell. After thorough degassing, Ar (60−80 Torr) was introduced into the cell. The photodecomposition of water was then carried out under irradiation of light from a high-pressure Hg lamp operated at 400 W (SEN, HL-400EH-5). H_2/O_2 gases evolved were analyzed by gas chromatography (Shimadzu, GC-8A, Ar gas carrier, MS-5A Column, TCD).

Results and Discussion

(a) Structural Evolution of $Sr_2Nb_xTa_{2-x}O_7$ and Powder Characterization. To determine the heat-treatment temperature for $Sr_2Nb_xTa_{2-x}O_7$ to be well-crystallized, the powder precursor for $Sr_2Ta_2O_7$ was heat-treated for 5 h at different temperatures between 700 and 1000 °C. The resulting XRD patterns are shown in Figure 2. It is clearly seen that a partial crystallization of $Sr_2Ta_2O_7$ has occurred during the heat treatment of the powder precursor at 850 °C for 5 h, and it was completed at temperatures higher than 900 °C. Figure 3 shows TEM photographs of powders obtained at (a) 800 °C and (b) 900 °C for 5 h, indicating that while the former (a) is a conglomerate consisting of a huge number of nanoparticles and not yet crystallized, in agreement with the XRD result (Figure 2), the latter (b) is well-crystallized with particle sizes of several hundred nanometers. We thus decided the preparation temperature for $Sr_2Nb_xTa_{2-x}O_7$ at 900 °C as is shown later. In this study, we do not try to determine the fraction of crystalline versus amorphous oxides in powders prior to the full crystallization, because no details such as composition and structures for the amorphous oxides are known in the $Sr_2Ta_2O_7$ system.

We have also examined the effect of heat-treatment times on the crystallization behavior of $Sr_2Ta_2O_7$ at a fixed temperature. The XRD patterns of $Sr_2Ta_2O_7$ powders prepared by the PC method at 800 °C for various heat-treatment times are shown in Figure 4. Time-dependent crystallization has occurred during the heat treatment at 800 °C from 5 to 48 h. TEM photographs of powders obtained at 800 °C for 24 and 48 h indicate that while the former consists of parts well-crystallized and those noncrystallized, the latter is completely crystallized. The XRD patterns of $Sr_2Ta_2O_7$ powders prepared at 700 °C showed that $Sr_2Ta_2O_7$ was not crystallized at 700 °C, even after the prolonged heat treatment up to 100 h.

Figure 5 shows the XRD patterns of $Sr_2Nb_xTa_{2-x}O_7$ ($x = 0-2$) powders prepared by the PC method at 900 °C for 5 h, confirming their single-phase nature for each composition. Of particular importance is that no reflections from $SrCO_3$, Nb_2O_5, and Ta_2O_5 were observed as distinct impurities, implying an improved mixing of the constituent cations in the PC-derived powder precursors. The PC method has a great advantage over the conventional SSR method in that a phase-pure compound can be prepared at reduced temperatures for a shorter reaction time. For instance, the PC method has produced phase-pure $Sr_2Ta_2O_7$ and $Sr_2Nb_2O_7$ at 900 °C for 5 h in this work, as opposed to the SSR method, in which firing at 1180 °C for 200 h and at 1100 °C for 150 h is required for phase-pure $Sr_2Ta_2O_7$ and $Sr_2Nb_2O_7$, respectively.[9] The crystal structure of both $Sr_2Ta_2O_7$ and $Sr_2Nb_2O_7$ possessing layered perovskite structures has been precisely solved by Ishizawa et al.[21,22] using single-crystal XRD data. Of particular interest is that the layered perovskite structure of $Sr_2Nb_2O_7$ is largely twisted, whereas $Sr_2Ta_2O_7$ takes an almost ideal structure. Unfortunately, our powder diffraction data do not allow us to solve the crystal structure of the solid solutions precisely, and we therefore skip further discussion related to the structural features of the solid solutions.

Another important characteristic of our $Sr_2Nb_xTa_{2-x}O_7$ powders prepared by the PC method is their relatively large surface areas when compared with those for samples obtained by the SSR method. Indeed, the specific surface areas of the PC-derived $Sr_2Ta_2O_7$ and $Sr_2Nb_2O_7$ at 900 °C were 7.3 and 4.3 $m^2 \cdot g^{-1}$, respectively, while those for $Sr_2Ta_2O_7$ and $Sr_2Nb_2O_7$ obtained by the SSR method were quite low, typically less than 1 $m^2 \cdot g^{-1}$.[9] Having a crystalline material with a larger surface area is of practical importance for certain applications, particularly a catalytic application. It can be anticipated that our PC-derived materials with high surface areas exhibit improved catalytic activities, the results of which are shown in Section c.

(b) Diffuse Reflection Spectra of $Sr_2Nb_xTa_{2-x}O_7$. The diffuse reflection spectra of $Sr_2Nb_xTa_{2-x}O_7$ prepared by the PC method at 900 °C are shown in Figure 6. The band gaps of PC-derived $Sr_2Ta_2O_7$ and $Sr_2Nb_2O_7$ were estimated to be 4.5 and 3.9 eV from onsets of the absorption, respectively, which are in good agreement with those obtained for the SSC-derived compounds.[9,24] It is noteworthy that the onset of the diffuse reflection spectra with the Nb substitution is not linearly shifted. The overall band gap of a given $Sr_2Nb_xTa_{2-x}O_7$ solid solution can be thought to depend mainly upon two

(24) Kato, H.; Kudo, A. *J. Photochem. Photobiol., A* **2001**, *145*, 129.

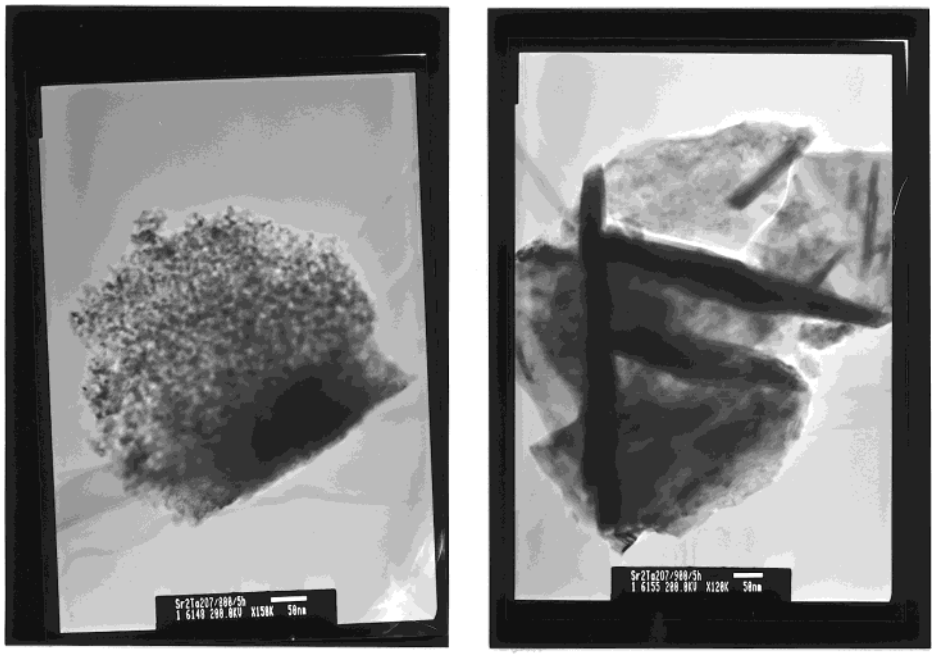

Figure 3. TEM images of $Sr_2Ta_2O_7$ synthesized by the polymerizable complex method at (a) 800 °C and (b) 900 °C for 5 h.

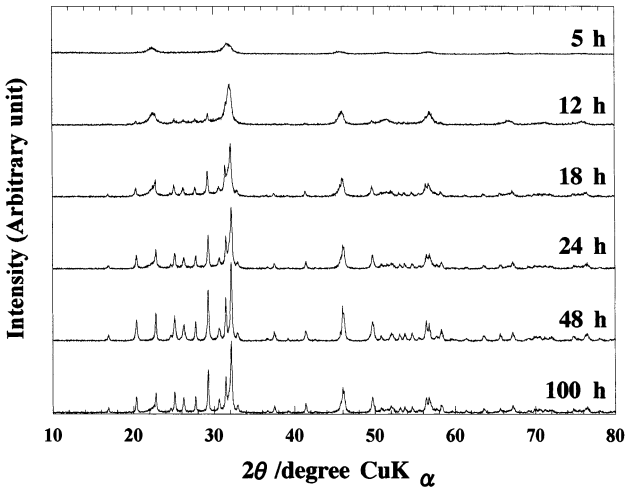

Figure 4. XRD patterns of $Sr_2Ta_2O_7$ synthesized by the polymerizable complex method at 800 °C for various heat-treatment times (5−100 h).

factors: (i) the degree of Ta_{5d} and Nb_{4d} orbitals being involved in the conduction band and (ii) the degree of delocalization of excitation energy due to the distortion of the crystal structure arising from Nb substitution. It may thus be said that change in the band gap energy is not necessarily proportional to that in the amount of the Nb substitution.

(c) Photocatalytic Activities of $Sr_2Nb_xTa_{2-x}O_7$ without NiO. Figure 7 shows H_2 and O_2 gas evolution rates (per gram) for naked $Sr_2Nb_xTa_{2-x}O_7$ ($x = 0-2$) prepared by the PC method at 900 °C for 5 h. One of the striking results is that the photocatalytic activity of $Sr_2Ta_2O_7$ ($x = 0$) was dramatically decreased by replacing tantalum with niobium. The large difference of the photocatalytic activity between $Sr_2Ta_2O_7$ and $Sr_2Nb_2O_7$ was explained in terms of the different conduction band levels formed by Ta_{5d} and Nb_{4d}.[9,24] However, the dramatic drop on photocatalytic activity induced by including such a low amount of Nb into $Sr_2Ta_2O_7$ cannot be accounted for solely by the difference in the conduction band level. This may be explained in conjunction with a lattice distortion around the niobium substituted.[24] Such a lattice distortion may act as a recombination center for photoinduced electron−hole pairs, leading to a dramatic drop on the photocatalytic activity. It is noteworthy that the solid solutions produced H_2 and O_2 nonstoichiometrically. In case of using a photocatalyst showing low activities, it is often observed that the amount of O_2 evolved becomes smaller than that expected from the stoichiometry (i.e., $H_2/O_2 = 2:1$). This would be due to the accumulation of oxidation products such as peroxides on the surface of the catalyst. Figure 8 shows the time course of H_2 and O_2 evolution over the $Sr_2Ta_2O_7$ photocatalyst, proving that H_2 and O_2 photocatalytically evolved steadily in a stoichiometric ratio except for the early data points after 1 h photolysis. Such a deviation would be again due to the accumulation of oxidation products on the surface of the catalyst. This phenomenon can be more pronounced in the early stages of photocatalytic evolution of H_2 and O_2 from water, because it takes time for the surface of the catalyst to be saturated by the oxidation products.

The photocatalytic activity data reported for $Sr_2Ta_2O_7$ and $Sr_2Nb_2O_7$ prepared by the SSR method[9] are also included in Figure 7, and they are compared in Table 1 with those for the corresponding samples prepared by the PC method. As is seen in Table 1 or Figure 7, a remarkable increase in the photocatalytic activity was obtained for $Sr_2Ta_2O_7$ when going from the SSR sample to the PC sample, while no significant difference in their photocatalytic activities was observed between the SSR− and the PC−$Sr_2Nb_2O_7$.

(d) Photocatalytic Activities of NiO/$Sr_2Nb_xTa_{2-x}O_7$. It is known that the photocatalytic activity of $Sr_2Ta_2O_7$ and $SrTa_2O_6$ prepared by the SSR method is

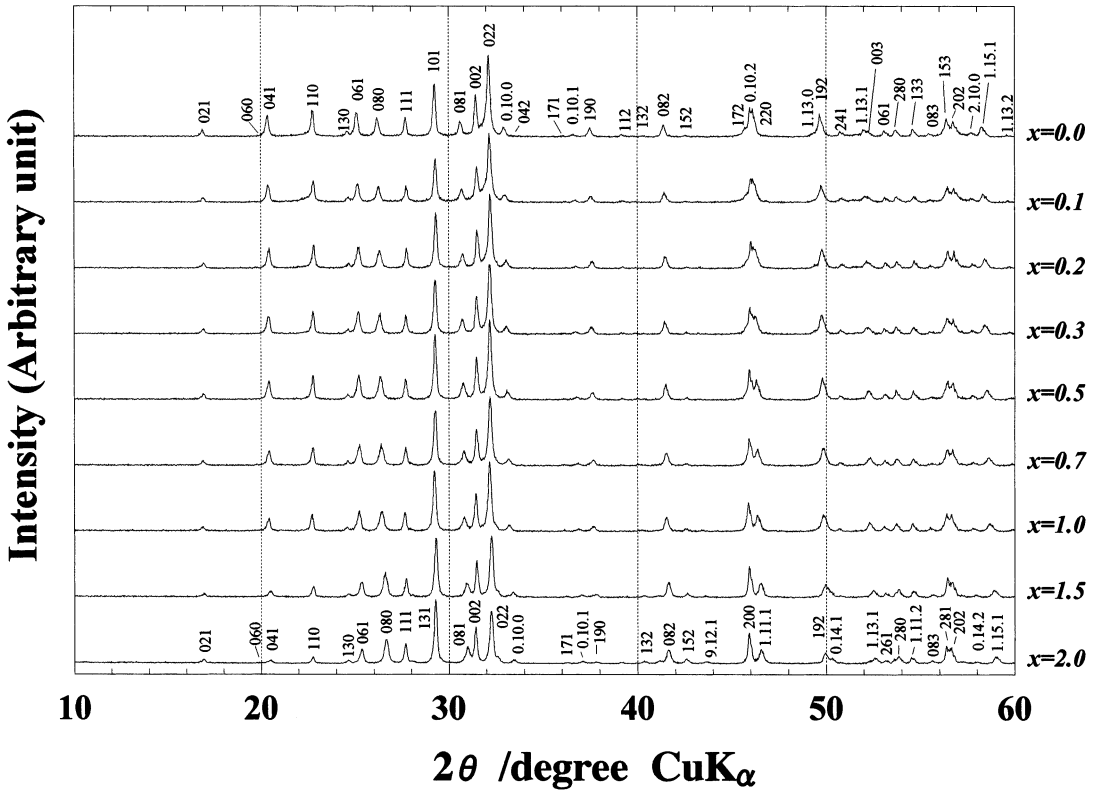

Figure 5. XRD patterns of $Sr_2Nb_xTa_{2-x}O_7$ ($x = 0-2$) synthesized by the polymerizable complex method at 900 °C for 5 h. Indexing for $Sr_2Ta_2O_7$ ($x = 0$) and $Sr_2Nb_2O_7$ ($x = 2$) is based upon the crystallographic data in refs *22* and *21*, respectively.

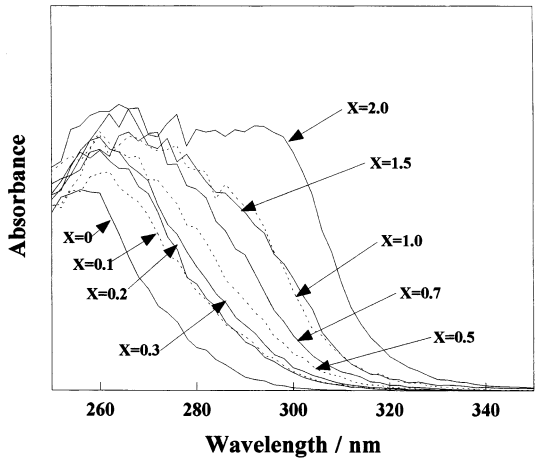

Figure 6. Diffuse reflectance spectra of $Sr_2Nb_xTa_{2-x}O_7$ synthesized by the polymerizable complex method at 900 °C for 5 h.

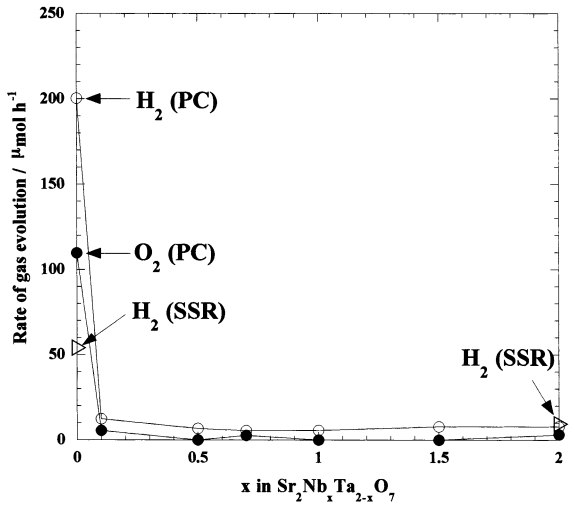

Figure 7. Effects of composition x on the photocatalytic activity for water decomposition over $Sr_2Nb_xTa_{2-x}O_7$ synthesized by the polymerizable complex method at 900 °C for 5 h ((○) H_2; (●) O_2). For comparison, the photocatalytic activity ((△) H_2) of $Sr_2Ta_2O_7$ ($x = 0$) and $Sr_2Nb_2O_7$ ($x = 2$) synthesized by the solid-state reaction method (ref *9*) is shown. The rate of gas evolution is expressed in units per gram of catalyst.

drastically increased by loading a NiO cocatalyst.[9] In this paper, effects of amounts of NiO cocatalyst on the photocatalytic activities of PC−$Sr_2Ta_2O_7$ were therefore investigated to determine the optimum amount of NiO loaded. Figure 9 shows the dependence of the photocatalytic activity for water decomposition over NiO/$Sr_2Ta_2O_7$ prepared by the PC method at 900 °C upon the amount of NiO loaded. The photocatalytic activity of $Sr_2Ta_2O_7$ was drastically increased upon NiO loading and showed a maximum at 0.15 wt % for the amount of NiO loaded. Figure 10 shows the time course of H_2 and O_2 evolution over NiO (0.15 wt %)/$Sr_2Ta_2O_7$, proving that H_2 and O_2 evolved in a stoichiometric ratio. The NiO (0.15 wt %)/$Sr_2Ta_2O_7$ photocatalyst showed very high activities with H_2 and O_2 evolution rates of 2787 and 1347 μmol·h^{-1}·g^{-1}, respectively, although the activities have a weak tendency to decrease slightly for the second run. The present photocatalytic data have been collected using the same equipment as that used in ref *9*, where a quantum yield of NiO (0.15 wt %)/$Sr_2Ta_2O_7$ prepared by the SSR method was reported. By taking the value of the quantum yield reported into account, the quantum yield of our NiO (0.15 wt %)/$Sr_2Ta_2O_7$ prepared by the PC method was estimated to be ~24% at 270 nm.

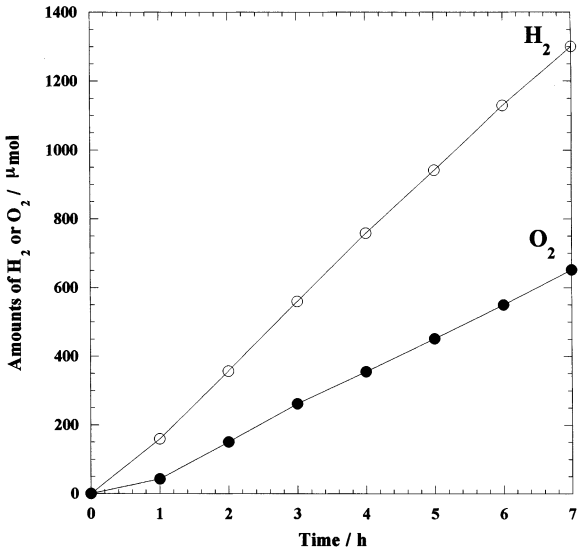

Figure 8. Time course of H_2 and O_2 evolution from pure water over $Sr_2Ta_2O_7$ synthesized by the polymerizable complex method at 900 °C for 5 h ((○) H_2; (●) O_2). Amounts of products are expressed in units per gram of catalyst.

Table 1. Photocatalytic Activities of $Sr_2Nb_2O_7$ and $Sr_2Ta_2O_7$ without NiO Prepared by the Conventional Solid-State Reaction (SSR)[a] and the Polymerizable Complex (PC) Method

catalyst	preparation method	BET surface area ($m^2 \cdot g^{-1}$)	rate of gas evolution[b] ($\mu mol \cdot h^{-1}$)	
			H_2	O_2
$Sr_2Nb_2O_7$	SSR method[a] 1100 °C, 150 h	0.7	5.9	0
	PC method 900 °C, 5 h	4.3	7.5	3.5
$Sr_2Ta_2O_7$	SSR method[a] 1180 °C, 200 h	0.9	52	18
	PC method 900 °C, 5 h	7.3	200	110

[a] Data from ref 9. [b] Expressed in units per gram of catalyst.

Figure 11 shows H_2 and O_2 gas evolution rates (per gram) for NiO (0.15 wt %)/$Sr_2Nb_xTa_{2-x}O_7$ ($x = 0-2$) photocatalysts. For comparison, the corresponding photocatalytic H_2 evolution data (Figure 7) for $Sr_2Nb_xTa_{2-x}O_7$ without NiO were also included in Figure 11. For all of the compositions, their photocatalytic activity was dramatically increased when the naked $Sr_2Nb_xTa_{2-x}O_7$ was loaded with NiO. NiO (0.15 wt %)/$Sr_2Ta_2O_7$ ($x = 0$) showed the highest activity among other compositions, and the activity was abruptly droped from $x = 0$ to 0.1 in a way similar to what has been observed for the naked $Sr_2Nb_xTa_{2-x}O_7$ photocatalysts. It should, however, be noticed that there has been a broad maximum in the photocatalytic activity at $x = 0.7$, the reason for which was recently accounted for by the suppressions of nonradiative transition.[24]

Table 2 compares photocatalytic activities of NiO-loaded $Sr_2Nb_2O_7$ and $Sr_2Ta_2O_7$ prepared by the PC method with those reported for samples prepared by the SSR method.[9] The PC method is obviously of greater advantage than the SSR method in that it produces photocatalysts with larger activities for shorter times at lower temperatures. Moreover, the NiO/PC−$Sr_2Nb_2O_7$ gave H_2 and O_2 in a stoichiometric ratio even without pretreatment, as opposed to what was obtained for the

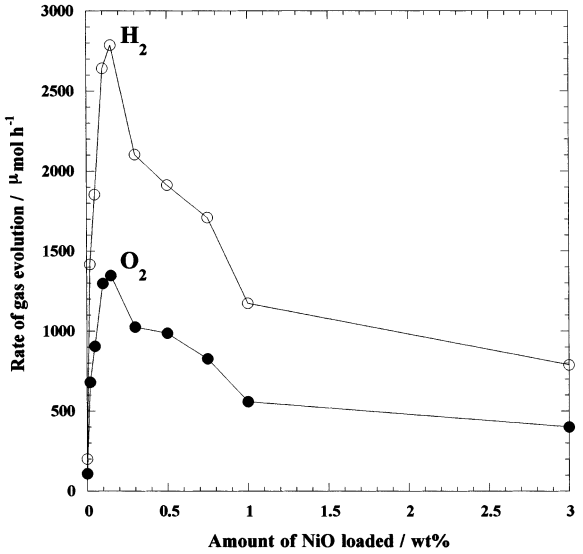

Figure 9. Effects of the amount of NiO loaded on the photocatalytic activity for water decomposition over NiO/$Sr_2Ta_2O_7$ synthesized by the polymerizable complex method at 900 °C for 5 h ((○) H_2; (●) O_2). The rate of gas evolution is expressed in units per gram of catalyst.

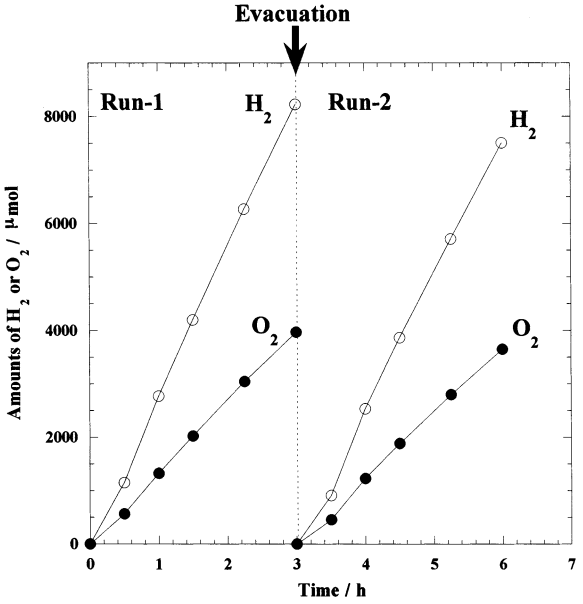

Figure 10. Time course of H_2 and O_2 evolution from pure water over NiO (0.15 wt %)/$Sr_2Ta_2O_7$ synthesized by the polymerizable complex method at 900 °C for 5 h ((○) H_2; (●) O_2). The gas phase was evacuated at 3 h after startup (Run 1), and the second run was subsequently started. Amounts of products are expressed in units per gram of catalyst.

corresponding NiO/SSR−$Sr_2Nb_2O_7$ (Table 2).[9] The relative photocatalytic activity of the NiO/SSR−$Sr_2Nb_2O_7$ was greatly improved when it was pretreated by H_2 reduction and subsequent O_2 oxidation (Table 2),[9] as has been carried out for other NiO-loaded photocatalysts.[25−31] However, we were still aware of the nonstoichiometric

(25) Kudo, A.; Domen, K.; Maruya, K.; Onishi, T. *Chem. Phys. Lett.* **1987**, *133*, 517.
(26) Domen, K.; Kudo, A.; Onishi, T. *J. Catal.* **1986**, *102*, 92.
(27) Kudo, A.; Sayama, K.; Tanaka, A.; Asakura, K.; Domen, K.; Maruya, K.; Onishi, T. *J. Catal.* **1989**, *120*, 337.
(28) Sayama, K.; Arakawa, H. *J. Photochem. Photobiol., A* **1994**, *77*, 243.
(29) Takata, T.; Furumi, Y.; Shinohara, K.; Tanaka, A.; Hara, M.; Kondo, J. N.; Domen, K. *Chem. Mater.* **1997**, *9*, 1063.

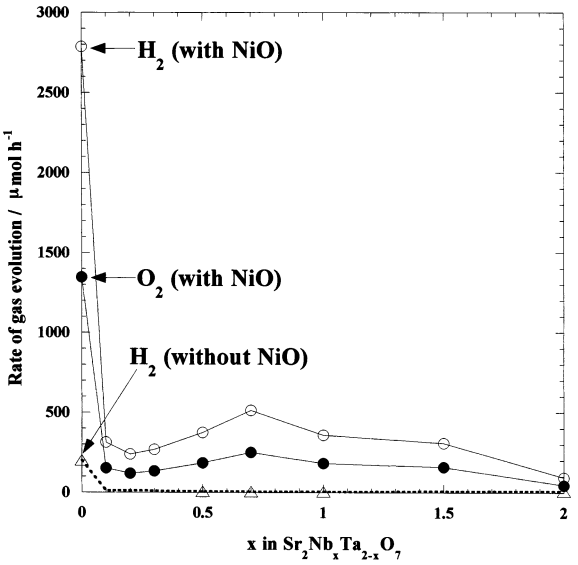

Figure 11. Effects of composition x on the photocatalytic activity for water decomposition over NiO (0.15 wt %)/Sr_2Nb_x-$Ta_{2-x}O_7$ synthesized by the polymerizable complex method at 900 °C for 5 h ((○) H_2; (●) O_2). For comparison, the corresponding photocatalytic activity ((△) H_2) for $Sr_2Nb_xTa_{2-x}O_7$ without NiO (data from Figure 12) is shown. The rate of gas evolution is expressed in units per gram of catalyst.

Table 2. Photocatalytic Activities of NiO/$Sr_2Nb_2O_7$ and NiO/$Sr_2Ta_2O_7$ Prepared by the Conventional Solid-State Reaction (SSR)[a] and the Polymerizable Complex (PC) Method

catalyst	preparation method	pre-treatment[b]	rate of gas evolution[c] (μmol·h^{-1}) H_2	O_2
NiO (0.15 wt %)/ $Sr_2Nb_2O_7$	SSR method[a] 1100 °C, 150 h	no	10	3.2
	SSR method[a] 1100 °C, 150 h	yes	110	36
NiO (0.15 wt %)/ $Sr_2Nb_2O_7$	PC method 900 °C, 5 h	no	94	46
NiO (0.15wt%)/ $Sr_2Ta_2O_7$	SSR method[a] 1180 °C, 200 h	no	1000	480
	PC method 900 °C, 5 h	no	2787	1347
	PC method 800 °C, 48 h	no	3517	1733

[a] Data from ref 9. [b] H_2 reduction at 500 °C for 2 h and subsequent oxidation at 200 °C for 1 h. [c] Expressed in units per gram of catalyst.

water decomposition by NiO/SSR−$Sr_2Nb_2O_7$ photocatalyst even after the pretreatment (Table 2).

(e) Effects of Preparation Temperature and Heat-Treatment Time on the Photocatalytic Activities of NiO (0.15 wt %)/$Sr_2Ta_2O_7$ Photocatalysts. Specific rates of the H_2 and O_2 gas evolution for NiO (0.15 wt %)/$Sr_2Ta_2O_7$ are plotted as a function of the preparation temperature in Figure 12, wherein data for the BET specific surface area of each sample are also included. NiO/$Sr_2Ta_2O_7$ samples prepared at a lower temperature range of 700−850 °C showed the photocatalytic activity of only 71−214 μmol·h^{-1}·g^{-1} for H_2 evolution, which are much less than those expected from

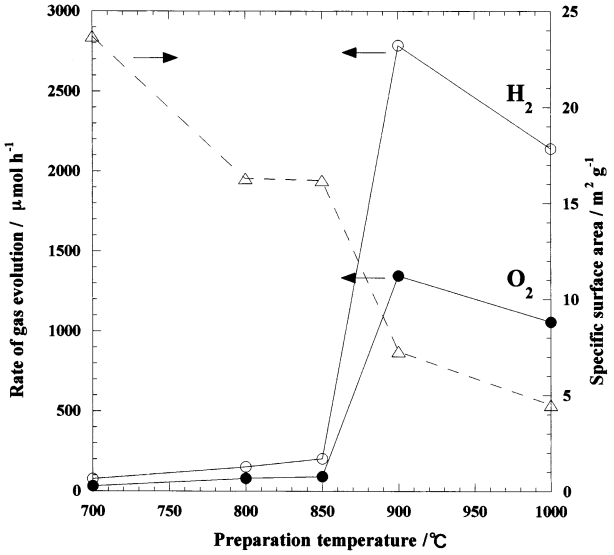

Figure 12. Rate of gas evolution ((○) H_2; (●) O_2) and the specific surface area (△) for NiO (0.15 wt %)/$Sr_2Ta_2O_7$ synthesized by the polymerizable complex method for 5 h as a function of preparation temperature. The rate of gas evolution is expressed in units per gram of catalyst.

their relatively large specific surface areas (23.7−16.2 m^2·g^{-1}). In a sharp contrast to this observation, the NiO/$Sr_2Ta_2O_7$ sample prepared at 900 °C produced H_2 with a large photocatalytic activity of 2787 μmol·h^{-1}·g^{-1} despite its smaller surface area (7.3 m^2·g^{-1}). The low photocatalytic activities of the samples prepared at temperatures below 850 °C are obviously related to their extremely poor crystallinity as was confirmed by their XRD (Figure 2) and TEM images (Figure 3).

Similarly, noncrystalline or poorly crystalline NiO/$Sr_2Ta_2O_7$ samples prepared at 800 °C for 5−12 h (see XRD patterns in Figure 4) showed relatively small photocatalytic activities of 153−257 μmol·h^{-1}·g^{-1} despite their large surface areas (16.3−13.6 m^2·g^{-1}). The photocatalytic activity of NiO/$Sr_2Ta_2O_7$ for H_2 evolution is increased rapidly from 257 to 3517 μmol·h^{-1}·g^{-1} when the heat-treatment time is increased from 12 to 48 h, while the corresponding surface area is moderately decreased from 13.6 to 10.7 m^2·g^{-1}. There are two conflicting factors that affect the overall photocatalytic activity in an opposite way (i.e., the number of lattice defects and the surface area).[32] Lattice defects may act as recombination centers for photoinduced electrons and holes, thus reducing the net photocatalytic activity significantly. The rapid increase in the photocatalytic activity when going from 12 to 48 h may therefore be understood in such a way that the number of lattice defects acting as inactivation centers is rapidly decreased as the heat-treatment time is increased. The idea that reactivities at a surface of a poorly crystallized material are suppressed by lattice defects acting as electron−hole traps was recently proposed by Ohtani et al.[33] for an amorphous anatase mixture of TiO_2 particles and by Stone et al.[34] for TiO_2 and Nb_2O_5 mesoporous molecular sieves.

(30) Ikeda, S.; Hara, M.; Kondo, J. N.; Domen, K.; Takahashi, H.; Okubo, T.; Kakihana, M. *J. Mater. Res.* **1998**, *13*, 852.
(31) Sayama, K.; Arakawa, H.; Domen, K. *Catal. Today* **1996**, *28*, 175.
(32) Heller, A.; Degani, Y.; Johnson, D. W.; Gallagher, P. K. *J. Phys. Chem.* **1987**, *91*, 5987.
(33) Ohtani, B.; Ogawa, Y.; Nishimoto, S. *J. Phys. Chem.* **1997**, *101*, 3746.
(34) Stone, V. F., Jr.; Davis, R. J. *Chem. Mater.* **1998**, *10*, 1468.

On the other hand, for well-crystalline materials practically free from lattice defects, the photocatalytic activity should be primarily governed by their surface area. The observation of the reduction in the photocatalytic activity with an increase in the preparation temperature from 900 to 1000 °C (Figure 12) can be attributed to the decrease in the surface area. Similarly, the decrease in the photocatalytic activity for H_2 evolution from 3517 to 1634 μmol·h^{-1}·g^{-1} with an increase in the heat-treatment time from 48 to 100 h can be partly explained in terms of a decrease in the specific surface area from 10.7 to 9.3 m^2·g^{-1}. The unusually large photocatalytic activity in the NiO (0.15 wt %)/$Sr_2Ta_2O_7$ prepared at 800 °C for 48 h for H_2 and O_2 evolution from pure water with specific rates of 3517 and 1733 μmol·h^{-1}·g^{-1} (see Table 2) can be explained as a consequence of obtaining such a well-optimized sample with respect to the balance between the number of lattice defects (related to the crystallinity) and the surface area.

Conclusion

Pure $Sr_2Nb_xTa_{2-x}O_7$ (SNT, $x = 0-2$) was successfully synthesized by heat treating the PC powder precursors at 900 °C for 5 h. The success in lowering the preparation temperature for SNT implies an improved level of mixing of cations in the powder precursors. The photocatalytic activity of SNT with and without NiO for the water decomposition into H_2 and O_2 under UV light irradiation did not scale simply with the specific surface area of the samples. It has been suggested that the high surface area alone does not guarantee high activity for poorly crystalline samples that contain a number of lattice defects and that such lattice defects may act as recombination centers for photoinduced electrons and holes, thus reducing the overall photocatalytic activity significantly. The two conflicting factors (i.e., the number of lattice defects and the specific surface area), which affect the overall photocatalytic activity in an opposite way, should be taken into consideration to obtain a photocatalyst with the highest activity. It is concluded that the PC route is a promising method for preparing highly active SNT photocatalysts for the water decomposition into H_2 and O_2, because the preparation temperature (typically 800−900 °C) in our PC synthesis of SNT is low enough to avoid unwanted large grain growth and high enough to fully crystallize SNT.

Acknowledgment. Helpful discussions with Professor Masahiro Yoshimura are greatly acknowledged. This work was financially supported by a Grant-in-Aid for Scientific Research (13450264).

CM0109037